

Revisiting Frequency Reuse towards Supporting Ultra-Reliable Ubiquitous-Rate Communication

Jihong Park, Dong Min Kim, Petar Popovski, and Seong-Lyun Kim[†]

Abstract—One of the goals of 5G wireless systems stated by the NGMN alliance is to provide moderate rates (50+ Mbps) everywhere and with very high reliability. We term this service *Ultra-Reliable Ubiquitous-Rate Communication (UR2C)*. This paper investigates the role of frequency reuse in supporting UR2C in the downlink. To this end, two frequency reuse schemes are considered: *user-specific* frequency reuse (FR_u) and *BS-specific* frequency reuse (FR_b). For a given unit frequency channel, FR_u reduces the number of serving user equipments (UEs), whereas FR_b directly decreases the number of interfering base stations (BSs). This increases the distance from the interfering BSs and the signal-to-interference ratio (SIR) attains ultra-reliability, e.g. 99% SIR coverage at a randomly picked UE. The ultra-reliability is, however, achieved at the cost of the reduced frequency allocation, which may degrade overall downlink rate. To fairly capture this reliability-rate tradeoff, we propose *ubiquitous rate* defined as the maximum downlink rate whose required SIR can be achieved with ultra-reliability. By using stochastic geometry, we derive closed-form ubiquitous rate as well as the optimal frequency reuse rules for UR2C.

Index Terms—UR2C, ultra-reliability, ubiquitous rate, user-specific frequency reuse, BS-specific frequency reuse, stochastic geometry

I. MOTIVATION AND CONTRIBUTION

Two extremes of 5G wireless system designs are pursuing very high data rate, i.e. enhanced mobile broadband (eMBB), and enabling ultra-reliable low-latency communication (URLLC) with very low data rate [1]–[3]. This paper explores a missing piece between them, *Ultra-Reliable Ubiquitous-Rate Communication (UR2C)*, answering to the question how much data rate can stably be achieved everywhere. For example, the NGMN Alliance suggests that a rate of at least 50 Mbps should be supported practically everywhere [1]. In this paper “practically” means that a randomly picked user equipment (UE) can ubiquitously attain a predefined data rate with 99% reliability, which is higher than the commonly considered 95% reliability of the wireless coverage [1], [3].

An important enabler of UR2C is ultra-dense base station (BS) deployment where BS/UE density ratio *per communication resource* exceeds 1 [4]. A larger density of BSs improves signal-to-interference ratio (SIR) since it increases the number of non-interfering BSs that have no serving UE within their

J. Park, D. M. Kim, and P. Popovski are with Department of Electronic Systems, Aalborg University, Denmark (email: {jihong, dm, petarp}@es.aau.dk).

[†]S.-L. Kim is with School of EEE, Yonsei University, Seoul, Korea (email: slkim@yonsei.ac.kr).

This work has been supported in part by the Danish Ministry of Higher Education and Science (EliteForsk Award, Grant Nr. 5137-00073B), and partly by the National Research Foundation of Korea (NRF) grant funded by the Korea government (MSIP) (NRF-2014R1A2A1A11053234).

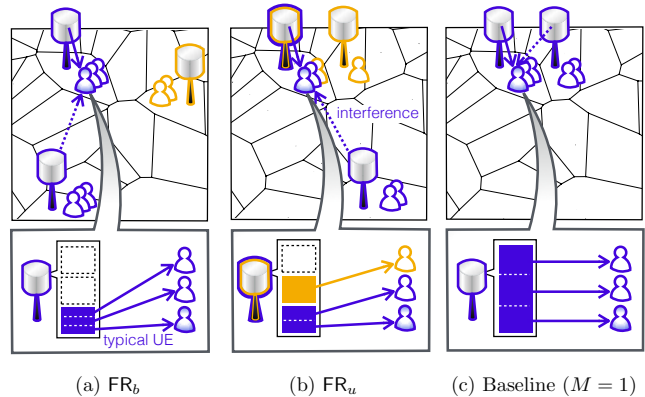


Fig. 1. Illustrations of FR_u and FR_b when the number of channels $M = 3$: (a) In FR_b , a BS randomly selects a single channel for all associated UEs; (b) In FR_u , a BS randomly assigns a single channel to each associated UE. At a typical UE (filled blue), both FR_b and FR_u thereby increase interfering BS distance, compared to (c) the baseline’s when $M = 1$.

cells. This makes the desired received signal power grow faster than the interference increase when deploying more BSs.

The effect of ultra-densification can also be achieved by dividing the total bandwidth into frequency channels. It makes interfering BSs located farther away, yielding SIR improvement. This motivated us to reconsider the problem of *frequency reuse*. In a downlink scenario, we fine-tune frequency reuse to make it applicable for a randomly selected UE, i.e. a *typical UE*. Thereby we aim at proposing an optimal frequency reuse scheme that achieves our target ultra-reliability, 99% SIR coverage. To this end, we suggest two frequency reuse techniques: *BS-specific* frequency reuse (FR_b) and *user-specific* frequency reuse (FR_u). When the entire frequency bandwidth is divided into M number of channels, each BS in FR_b uses only a single channel that it selects randomly (see Fig. 1-a). In FR_u , a BS randomly assigns a single channel to each associated UE (Fig. 1-b). If all the assigned channels to UEs are not identical, its corresponding BS utilizes multiple number of channels. Nevertheless, average amount of FR_u ’s channel use is still less than a baseline without frequency reuse, i.e. $M = 1$ (Fig. 1-c). As every scheme with M larger than 1, both FR_b and FR_u introduce loss in the data rate as they are only partially using the bandwidth.

To make the proposed schemes applicable not only for a cell-edge UE but also for a typical UE, it is therefore important to examine how much data rate degrades in return for reliability improvement. For this purpose, we propose *ubiquitous rate* \mathcal{R}_η defined as the maximum ergodic capacity

that guarantees a target η SIR coverage probability for a given SIR threshold t . For instance, $\mathcal{R}_{0.99}$ for unit resource allocation is $0.99 \cdot \log_2(1+t)$ bps, where t is given by taking the inverse function of SIR coverage probability to the target *reliability constraint equation* $\Pr(\text{SIR} \geq t) = 0.99$.

In this respect, we utilize stochastic geometry, and provide the closed-form downlink ubiquitous rate at a typical UE. Its derivation follows in part from preceding works that provide closed-form downlink SIR coverage at a typical UE in a form of a hypergeometric function [5], [6]. However, inverting a hypergeometric function to solve the reliable constraint equation is not analytically viable. We instead propose novel closed-form SIR bounds by using a hypergeometric function transformation technique, and thereby derive the desired ubiquitous rate in a closed form. Based on this result, we optimize FR_b and FR_u with respect to M , and investigate how to achieve the UR2C's target 50 Mbps ubiquitous rate with 99% reliability under different deployment density scenarios.

The contributions of this paper are summarized as follows.

- Optimized frequency reuse designs for UR2C are proposed (see **Proposition 3** with Figs. 3 and 4).
- Closed-form ubiquitous rates and SIR reliabilities under the frequency reuse schemes are derived (**Proposition 2**).
- Closed-form SIR reliability approximation for UR2C as well as closed-form SIR reliability bounds are provided (**Lemmas 2** and **3**).

II. SYSTEM MODEL

In a downlink cellular network, BSs are uniformly distributed with density λ_b , resulting in a homogeneous Poisson point process (PPP). Independently, UEs are also uniformly distributed with density λ , leading to another homogeneous PPP with density λ . Each UE associates with the nearest BS, forming a Poisson-Voronoi tessellation [7].

The entire frequency bandwidth W is divided into M_i channels, where hereafter the subscript $i \in \{b, u, o\}$, respectively, denotes FR_b , FR_u , and a baseline model. In FR_b , each BS randomly selects a single frequency channel, and serves its associated UEs only via the selected channel. In FR_u , a BS randomly assigns a single channel to each of its associated UE, and serves them respectively through the UEs' assigned channels. In the baseline, BSs neglect frequency reuse, and serve their associated UEs by using the entire bandwidth, i.e. $M_o = 1$. For all cases, multiple UEs using the same bandwidth are served by the BS through an equal TDMA allocation.

A BS occupies each channel when at least a single UE is served via the channel; otherwise, the channel remains void for that BS and the BS is considered inactive. For λ density of UEs served by a BS via a single channel, the BS's corresponding *channel occupancy probability* $p_c(\lambda)$ is given as $p_c(\lambda) \approx 1 - (1 + \lambda/[3.5\lambda_b])^{-3.5}$ [8], which is a monotone increasing (or decreasing) function of λ (or λ_b). In sparse networks $\lambda_b/\lambda \rightarrow 0$, $p_c(\lambda)$ becomes 1, while for ultra-dense networks $\lambda_b/\lambda \rightarrow \infty$, $p_c(\lambda)$ decreases towards 0 at the rate λ/λ_b [4].

For each non-void channel, a BS allocates unity power, and transmits signals. The transmitted signals experience path-loss

TABLE I
LIST OF NOTATIONS

Notation	Meaning
FR_b, FR_u	BS/User-centric frequency reuse
W	Total frequency bandwidth
M_i	# Channels where $i \in \{b, u, o\}$ resp. for FR_b , FR_u and baseline
$\text{SIR}(M_i)$	SIR under M_i number of channels
N_i	# UEs sharing the same BS and channel with a typical UE
$\mathcal{P}_t(M_i)$	SIR reliability with SIR threshold t
η	Target SIR reliability; e.g. 0.99 for 99% SIR reliability
$R_t(M_i)$	Average rate, given as $W/M_i \cdot \mathbb{E}[1/N_i] \cdot \log_2(1+t)$
$\mathcal{R}_\eta(M_i)$	Ubiquitous rate, maximum average rate s.t. $\mathcal{P}_t(M_i) \geq \eta$
λ_b, λ	BS and UE densities
$p_c(\lambda)$	Channel occupancy probability for serving UE density λ

attenuation with the exponent $\alpha > 2$ and Rayleigh fading with unit mean. Noise power is assumed to be much smaller than interference, and is thus neglected as in [4]–[6].

III. PROBLEM FORMULATION: UBIQUITOUS RATE MAXIMIZATION

At a typical UE, the reliability of SIR $\mathcal{P}_t(M_i)$ when there are M_i channels is defined as:

$$\mathcal{P}_t(M_i) := \Pr(\text{SIR}(M_i) \geq t) \quad (1)$$

where $\text{SIR}(M_i)$ is the SIR with M_i , elaborated in Section IV. Note that $\mathcal{P}_t(M_i)$ is a monotone increasing function of M_i . As M_i increases, interfering BSs become located farther away, which thereby improves $\text{SIR}(M_i)$ and so does $\mathcal{P}_t(M_i)$.

Increasing M_i , however, may decrease data rate since it reduces per-UE resource allocation at least by M_i . Precisely, the typical UE's downlink rate $R_t(M_i)$ is given as

$$R_t(M_i) := \underbrace{\frac{W}{M_i}}_{\text{resource allocation}} \cdot \mathbb{E}\left[\frac{1}{N_i}\right] \cdot \underbrace{\log_2(1+t)}_{\text{spectral efficiency}} \quad (2)$$

where N_i is the number of UEs served by the same BS via the same channel as the typical UE's.

The first term of resource allocation W/M_i in (2) indicates the maximum resource allocation per UE when a BS serves only a single UE, which is reduced by $1/M_i$. The actual resource allocation to a typical UE is $\mathbb{E}[1/N_i]$ portion of W/M_i since the maximum amount is equally allocated to the multiple UEs sharing the same channel and BS with the typical UE's. According to [8], the reciprocal of $\mathbb{E}[1/N_i]$ can be calculated by multiplying (i) the density of common UEs using the same channel as the typical UE's and (ii) average cell size of the BSs serving such common UEs. In FR_b , each BS utilizes only a single channel, so the entire UEs with density λ become the common UEs. Next, the density of the BSs serving the common UEs is $p_c(\lambda)\lambda_b$. The average size of cells having the common UEs then becomes $1/(p_c(\lambda)\lambda_b)$ because the average cell size of BSs is the reciprocal of the BS density [9]. As a result, $\mathbb{E}[1/N_b] = p_c(\lambda)\lambda_b/\lambda$. In the baseline, common UE density is also λ , so the same calculation applies, i.e. $\mathbb{E}[1/N_o] = \mathbb{E}[1/N_b]$. In FR_u , common UE density is

TABLE II
LIST OF RESOURCE ALLOCATION AND INTERFERER DENSITY

Scheme	Resource Allocation		Interferer Density λ_i
	W/M_i	$E[1/N_i]$	
Baseline	W	$p_c(\lambda)\lambda_b/\lambda$	$p_c(\lambda)\lambda_b$
FR _b	W/M_b	$p_c(\lambda)\lambda_b/\lambda$	$p_c(\lambda)\lambda_b/M_b$
FR _u	W/M_u	$p_c(\lambda/M_u)\lambda_b/(\lambda/M_u)$	$p_c(\lambda/M_u)\lambda_b$

reduced by $1/M_u$, and this enlarges the average cell size by replacing λ with λ/M_u , as summarized in Table II.

Consequently, in return for resource allocation reduction as M_i increases, it improves SIR reliability in (1), and thereby increases spectral efficiency in (2) for a fixed target reliability. To achieve UR2C, we capture this reliability-rate tradeoff between (1) and (2), and formulate our optimization problem.

$$\begin{aligned} \text{(P0) maximize } & R_t(M_i) \\ & \text{s.t. } \mathcal{P}_t(M_i) \geq \eta \end{aligned}$$

It is noted that $R_t(M_i)$ and $\mathcal{P}_t(M_i)$ respectively are monotone increasing and decreasing functions of the SIR threshold t . Therefore $R_t(M_i)$ is maximized when $\mathcal{P}_t(M_i) = \eta$ holds, which is the *reliability constraint equation*. In this respect, we define *ubiquitous rate* $\mathcal{R}_\eta(M_i)$ as the maximum rate guaranteeing $\mathcal{P}_t(M_i) \geq \eta$.

Our objective is to derive $\mathcal{R}_\eta(M_i)$ for each frequency reuse scenario. To this end, we first derive a closed-form $\mathcal{P}_t(M_i)$ approximation (Lemma 3), and thereby easily solve the reliability constraint equation with respect to t . For this given optimal t , we tractably optimize $\mathcal{R}_\eta(M_i)$ with respect to M_i under an ultra-reliable regime, i.e. $\eta \approx 1$.

IV. CLOSED-FORM RELIABILITY VIA NORMALIZED SIR

This section derives closed-form SIR reliability approximation for UR2C (Lemma 3). This enables closed-form ubiquitous rate expressions in the next section (Proposition 2). To this end, we consider the following two techniques.

Technique #1. SIR normalization. At a typical UE, let $S(\lambda_b)$ denote its received desired signal power when associating with the nearest BS out of all BSs with density λ_b . Similarly, $I_r(\lambda_i)$ denotes aggregate interference where λ_i is *interferer density* and r the typical UE's association distance. In the baseline utilizing the entire bandwidth, all the BSs that have at least a single UE perform downlink transmissions interfering with the typical UE. Therefore, $\lambda_o = p_c(\lambda)\lambda_b$. In FR_b, $1/M_b$ portion of such non-void BSs become interferers, and thus $\lambda_b = p_c(\lambda)\lambda_b/M_b$. In FR_u, only the BSs having at least a single UE that is served through the same channel as the typical UE's with probability $1/M_u$ become interferers. It leads to $\lambda = p_c(\lambda/M_u)\lambda_b$, as summarized in Table II.

Next, we utilize a transformation between BS density λ_b and received signal power $S(\lambda_b)$ (or λ_i and $I_r(\lambda_i)$). According to mapping theorem [7], P times transmission power increase for all BSs is almost surely (*a.s.*) identical to $P^{\frac{2}{\alpha}}$ times BS densification without their power increase, from the typical

UE's received signal power point of view. By exploiting this relationship, we can transform any $\text{SIR}(M_i) = S(\lambda_b)/I_r(\lambda_i)$ into its normalized value $\widetilde{\text{SIR}} = S(1)/I_r(1)$ specified in the following lemma.

Lemma 1. (SIR normalization, Corollary 2.35 in [7]) $\text{SIR}(M_i)$ and its normalized $\widetilde{\text{SIR}}$ satisfy the following relationship.

$$\text{SIR}(M_i) = \left(\frac{\lambda_b}{\lambda_i}\right)^{\frac{\alpha}{2}} \widetilde{\text{SIR}} \quad \text{a.s.} \quad (3)$$

This allows us to focus only on λ_i when examining the proposed scheme's impact on SIR.

Technique #2. Hypergeometric function transformation.

When $\lambda_i = \lambda_b$, it has been known that the baseline model's downlink SIR coverage at a typical UE is the reciprocal of a Gauss-hypergeometric function [5], [6], given as

$$\mathcal{P}_t(M_i) = {}_2F_1\left(1, -\frac{2}{\alpha}; 1 - \frac{2}{\alpha}; -t\right)^{-1} \quad (4)$$

where a Gauss hypergeometric function ${}_2F_1(a, b; c; z) := \sum_{n=0}^{\infty} \frac{(a)_n (b)_n z^n}{(c)_n n!}$ and Pochhammer symbol $(x)_n$ is defined as $\Gamma(x+n)/\Gamma(x)$ for the Gamma function $\Gamma(x+1) := x!$.

Applying Lemma 1 generalizes this result for an arbitrary $\lambda_i > 0$ by using Lemma 1.

$$\mathcal{P}_t(M_i) = \Pr\left(\widetilde{\text{SIR}} \geq \left[\frac{\lambda_i}{\lambda_b}\right]^{\frac{\alpha}{2}} t\right) \quad (5)$$

$$= {}_2F_1\left(1, -\frac{2}{\alpha}; 1 - \frac{2}{\alpha}; -\left[\frac{\lambda_i}{\lambda_b}\right]^{\frac{\alpha}{2}} t\right)^{-1} \quad (6)$$

The last step follows from (4), which is also applicable for $\widetilde{\text{SIR}}$. Setting $\lambda_i = \lambda_b = 1$ while replacing t with $(\lambda_i/\lambda_b)^{\frac{\alpha}{2}} t$ yield such a result.

The result (6) is, however, still not applicable for analytically solving the reliability constraint equation $\mathcal{P}_t(M_i) = \eta$ since the inverse function of (6) is unknown. We detour this problem by utilizing Pfaff's Gauss-hypergeometric function transformation [10], specified in the following lemma.

Lemma 2. (Reliability Bounds) SIR *reliability* $\mathcal{P}_t(M_i)$ is upper and lower bounded as follows.

$$\frac{\alpha}{2\pi \csc\left(\frac{2\pi}{\alpha}\right)} \left(1 + \left[\frac{\lambda_i}{\lambda_b}\right]^{\frac{\alpha}{2}} t\right)^{-\frac{2}{\alpha}} \leq \mathcal{P}_t(M_i) \leq \left(1 + \left[\frac{\lambda_i}{\lambda_b}\right]^{\frac{\alpha}{2}} t\right)^{-\frac{2}{\alpha}} \quad (7)$$

Proof: Consider Pfaff's transformation [10] given as follows.

$${}_2F_1(c-a, b; c; [1-1/z]^{-1}) = (1-z)^{-b} {}_2F_1(a, b; c; z) \quad (8)$$

Setting $x = t(\lambda_i/\lambda_b)^{\frac{\alpha}{2}}$ and applying $a = b = -\frac{2}{\alpha}$, $c = 1 - \frac{2}{\alpha}$, and $z = (1+1/x)^{-1}$ yields $\mathcal{P}_t(M_i) = c_0(1+x)^{-\frac{2}{\alpha}}$ where $c_0 := {}_2F_1\left(-\frac{2}{\alpha}, -\frac{2}{\alpha}; 1 - \frac{2}{\alpha}; \frac{1}{1+x}\right)$ is a monotonically decreasing function of x , having maximum $\frac{2\pi}{\alpha} \csc\left(\frac{2\pi}{\alpha}\right)$ and minimum 1 respectively when x approaches 0 and ∞ . Applying these inequalities provides the desired result. ■

As shown in Fig. 2, the lower bound in Lemma 2 is only accurate for low SIR reliability when $t \rightarrow \infty$, so is not applicable for UR2C design. On the contrary, the upper bound

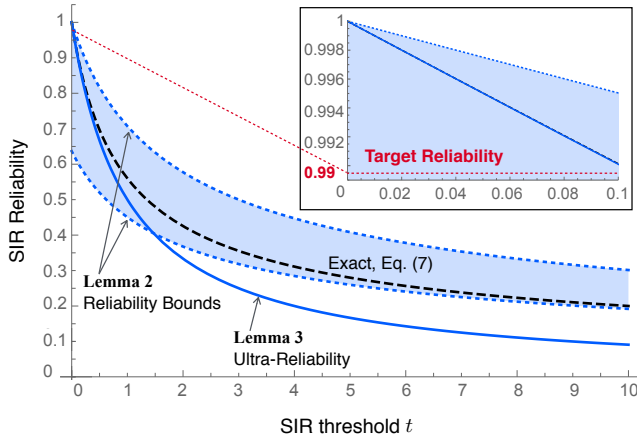


Fig. 2. Reliability bounds in Lemmas 2 and 3 ($\lambda_i = \lambda_b$, $\alpha = 4$).

has potential for the use in an ultra-reliable regime. This motivates us to further improve the upper bound.

With this end, we modify the upper bound so that it can asymptotically converge to the exact curve in the ultra-reliable regime, i.e. $t \rightarrow 0$. This only requires replacing the outermost exponent $2/\alpha$ with $2/(\alpha-2)$, leading to another lower bound.

Lemma 3. (Closed-Form Ultra-Reliability) SIR reliability $\mathcal{P}_t(M_i)$ is lower bounded as follows.

$$\mathcal{P}_t(M_i) \geq \left(1 + \left[\frac{\lambda_i}{\lambda_b}\right]^{\frac{\alpha}{2}} t\right)^{-\frac{2}{\alpha-2}} \quad (9)$$

where the equality holds when $(\lambda_i/\lambda_b)^{\frac{\alpha}{2}} t \rightarrow 0$

Proof: See Appendix. ■

As Fig. 2 shows, Lemma 3 lower bound is accurate in an ultra-reliable regime. In the following we therefore utilize this as an approximation, i.e. $\mathcal{P}_t(M_i) \approx \left(1 + [\lambda_i/\lambda_b]^{\frac{\alpha}{2}} t\right)^{-\frac{2}{\alpha-2}}$.

V. UBIQUITOUS RATE WITH FREQUENCY REUSE

In the first subsection, closed-form ubiquitous rates for FR_b and FR_u are derived. Based on this result, FR_b and FR_u are optimized in the second subsection.

A. Closed-Form Ubiquitous Rate

Applying Lemma 3 with λ_i summarized in Table II yields the closed-form reliabilities for FR_b , FR_u , and the baseline.

Proposition 1. (Reliability) For $\eta \approx 1$, the reliabilities of FR_b , FR_u , and the baseline for SIR threshold t are given as follows.

$$\text{FR}_b : \mathcal{P}_t(M_b) \approx \left[1 + \left(\frac{p_c(\lambda)}{M_b}\right)^{\frac{\alpha}{2}} t\right]^{-\frac{2}{\alpha-2}} \quad (10)$$

$$\text{FR}_u : \mathcal{P}_t(M_u) \approx \left[1 + p_c\left(\frac{\lambda}{M_u}\right)^{\frac{\alpha}{2}} t\right]^{-\frac{2}{\alpha-2}} \quad (11)$$

$$\text{Baseline} : \mathcal{P}_t(1) \approx \left[1 + p_c(\lambda)^{\frac{\alpha}{2}} t\right]^{-\frac{2}{\alpha-2}} \quad (12)$$

The closed-form representations makes it possible to invert the reliability constraint equation $\mathcal{P}_t(M_i) = \eta$ with respect

to t . Applying this t to the rate $R_t(M_i)$ in (2) leads to the following closed-form ubiquitous rates.

Proposition 2. (Ubiquitous Rate) For $\eta \approx 1$, ubiquitous rates of FR_b , FR_u , and the baseline are given as follows.

$$\text{FR}_b : \mathcal{R}_\eta(M_b) \approx \frac{\eta W p_c(\lambda) \lambda_b}{M_b \lambda} \log_2 \left(1 + \frac{c_\eta M_b^{\frac{\alpha}{2}}}{p_c(\lambda)^{\frac{\alpha}{2}}}\right) \quad (13)$$

$$\text{FR}_u : \mathcal{R}_\eta(M_u) \approx \frac{\eta W p_c\left(\frac{\lambda}{M_u}\right) \lambda_b}{\lambda} \log_2 \left(1 + \frac{c_\eta}{p_c\left(\frac{\lambda}{M_u}\right)^{\frac{\alpha}{2}}}\right) \quad (14)$$

$$\text{Baseline} : \mathcal{R}_\eta(1) \approx \frac{\eta W p_c(\lambda) \lambda_b}{\lambda} \log_2 \left(1 + \frac{c_\eta}{p_c(\lambda)^{\frac{\alpha}{2}}}\right) \quad (15)$$

where $c_\eta := \left(\frac{\alpha}{2} - 1\right) (1 - \eta)$

Proof: See Appendix. ■

This result specifies the impacts of frequency reuse and ultra-densification on ubiquitous rate as below.

Remark 1. (Impact of M_i) A larger M_i decreases resource allocation, and yet increases spectral efficiency. Therefore, optimizing M_i is required.

For FR_u , the foregoing remark comes from the fact that $p_c(\lambda/M_u)$ is a monotone decreasing function of M_u .

Remark 2. (Impact of Densification) BS densification improves both spectral efficiency and resource allocation.

By the definition $p_c(\lambda)$ decreases with λ_b , and asymptotically converges toward 0 at the rate of λ/λ_b . This makes the density of the BSs occupying a single channel is upper bounded by the entire UE density, i.e. $p_c(\lambda)\lambda_b \leq \lambda$. Until reaching this bound, BS densification at least provides a marginal gain in resource allocation. Deploying more BSs also increases spectral efficiency by improving SIR reliability as specified in Lemma 3, leading to the above remark.

Remark 3. (Indistinguishable Condition) The ubiquitous rates of FR_b and FR_u are indistinguishable if M_b and M_u satisfy $p_c(\lambda/M_u) = p_c(\lambda)/M_b$, which is not always ensured since M_u and M_b are integers no smaller than 1.

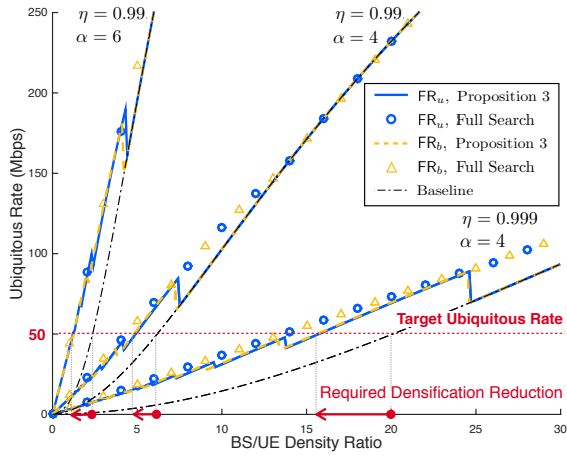
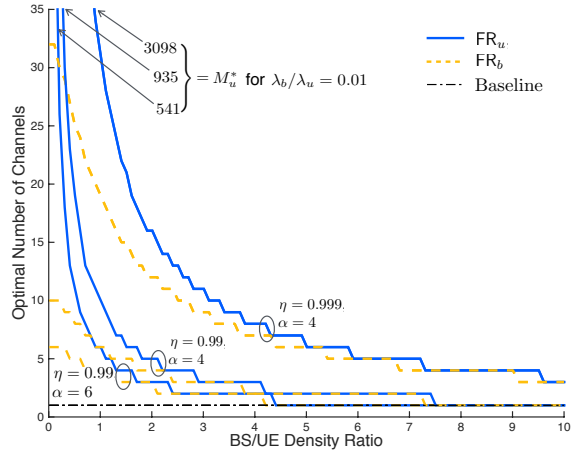
It straightforwardly follows from comparing (13) and (14). This remark predicts that the optimal ubiquitous rates of FR_b and FR_u are not always identical yet very close to each other, to be verified by simulation in the next section.

Remark 4. (Identically Optimal Condition) For the optimal M_i^* maximizing its ubiquitous rate, the optimal ubiquitous rates $\mathcal{R}_\eta(M_b^*)$ and $\mathcal{R}_\eta(M_u^*)$ become identical when both $M_b^*, M_u^* \rightarrow 1$ or $\lambda_b \rightarrow \infty$.

The case $M_i^* \rightarrow 1$ makes FR_b and FR_u converge to the baseline having $M_o = 1$. For $\lambda_b \rightarrow \infty$, indistinguishable condition in Remark 3 is always satisfied since $p_c(\lambda)$ and $p_c(\lambda/M_u)$ converge to 0.

B. Optimal Frequency Reuse Design

The optimal M_i^* maximizing the ubiquitous rate is found as follows.


 Fig. 3. Maximized ubiquitous rates of FR_b and FR_u ($W = 100$ MHz).

 Fig. 4. Maximized ubiquitous rates of FR_b and FR_u ($W = 100$ MHz).

Proposition 3. (Optimal M_i^*) For $\eta \approx 1$, the optimal M_i^* maximizing $\mathcal{R}_\eta(M_i)$ is given as below.

$$M_b^* \approx \arg \min_{M_b} \left| \left(1 + \frac{p_c(\lambda)^{\frac{\alpha}{2}}}{c_\eta M_b^{\frac{\alpha}{2}}} \right) \log_2 \left(1 + \frac{c_\eta M_b^{\frac{\alpha}{2}}}{p_c(\lambda)^{\frac{\alpha}{2}}} \right) - \frac{\alpha}{2} \right| \quad (16)$$

$$M_u^* \approx \arg \min_{M_u} \left| \left[c_\eta + p_c \left(\frac{\lambda}{M_u} \right)^{\frac{\alpha}{2}} \right] \log_2 \left(1 + \frac{c_\eta}{p_c \left(\frac{\lambda}{M_u} \right)^{\frac{\alpha}{2}}} \right) - \frac{\alpha c_\eta}{2} \right| \quad (17)$$

Proof: See Appendix. ■

For $\lambda_b \rightarrow 0$ or ∞ , the optimal M_i^* 's converge as follows.

Corollary 1. (Asymptotically Optimal M_i^*) For $\eta \approx 1$, the asymptotic behavior of the optimal M_i^* with respect to BS density λ_b is given as follows.

$$M_b^* = M_u^* = \begin{cases} \infty & \text{if } (1-\eta)\lambda_b^{\frac{\alpha}{2}} \rightarrow 0 \\ 1 & \text{if } (1-\eta)\lambda_b^{\frac{\alpha}{2}} \rightarrow \infty \end{cases} \quad (18)$$

In the first diverging M_i^* , we can notice that the increase in M_i^* comes from a higher reliability requirement η and/or lower BS density. This implies exploiting frequency reuse becomes more effective for the UR2C design in sparse networks. The second converging M_i^* to unity follows from the fact that BS ultra-densification can solely provide the target ultra-reliability while no longer relying on frequency reuse.

VI. NUMERICAL EVALUATION

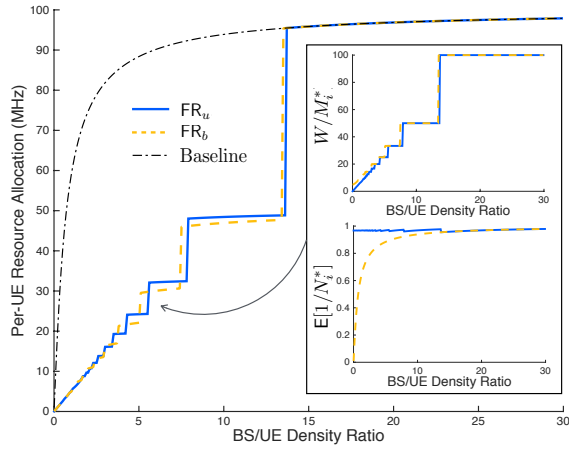
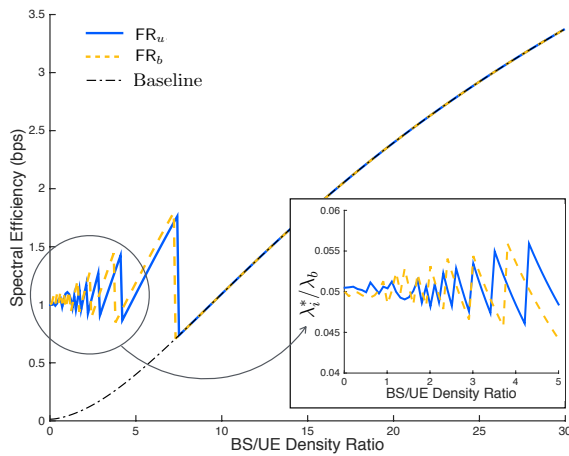
Default system parameters in this section are given as follows: $\eta = 0.99$, $\alpha = 4$, and $W = 100$ MHz [2]. Applying Proposition 3 to Proposition 2 via numerical simulation yields the following frequency reuse design guideline for UR2C.

FR_b and FR_u increases ubiquitous rate, further improved by higher η and α . Fig. 3 shows the maximized ubiquitous rates with FR_b and FR_u based on Proposition 3 (see yellow dotted and blue solid curves) outperform the baseline result without frequency reuse (black dash-dotted). The gain in ubiquitous rate, $\mathcal{R}_\eta(M_i^*)/\mathcal{R}_\eta(1)$, increases for higher η as it makes frequency reuse more effective to cope with the

target reliability requirement. Compared to the baseline, the maximum gain with $\eta = 0.999$ is 3.15 times larger than the gain with $\eta = 0.99$. For higher α , the gain also increases since SIR grows along with α under an interference-limited regime [4]–[6], amplifying the effect of frequency reuse in ubiquitous rate improvement. When α becomes 6 from 4, it increases the gain by 2.03 times. For a given target ubiquitous rate 50 Mbps, both FR_b and FR_u improve ubiquitous rate for all considered scenarios, while not converging to the baseline. This leads to reducing the required BS densification by up to 46%.

FR_b mostly performs better while FR_u sometimes outperforms for large BS density. Overall, the maximized ubiquitous rates of FR_b and FR_u keep crossing as BS density increases, but have no significant gap. As predicted in Remark 3, the reason follows from the fact that M_i^* 's are integers no smaller than 1. These coarse unit changes cannot effectively minimize the objective argument functions in Proposition 3, so constantly lead to peaky crossings as well as the gap between the results from Proposition 3 and a full search algorithm in Fig. 3, until FR_b and FR_u converge to the baseline. While having similar ubiquitous rates, FR_b requires less number of channels as shown in Fig. 4, so is more preferable than FR_u , especially for small BS density where M_u^* is unrealistically large. For moderate BS density, FR_u sometimes provides up to 28% higher ubiquitous rate than FR_b , and it is thus important to compare them in this regime for UR2C design. For large BS density, frequency reuse gain in ubiquitous rate disappears as also anticipated in Remark 4 and Corollary 1.

Optimal FR_b and FR_u provides similar per-UE resource allocations and spectral efficiencies. Fig. 5 illustrates that FR_b 's maximum per-UE allocation W/M_b^* is larger but its actual allocation fraction $E[1/N_b^*]$ within the maximum value due to multiple access is smaller. These two factors cancelled out each other, resulting in almost the same resource allocation as FR_u 's. Fig. 6 visualizes FR_b 's maximized spectral efficiency keeps crossing but becomes clearly larger under a small BS/UE density environment. This originates from the fact that FR_b more aggressively reduces interference by forcing to use only a


 Fig. 5. Maximized ubiquitous rates of FR_b and FR_u ($W = 100$ MHz).

 Fig. 6. Maximized ubiquitous rates of FR_b and FR_u ($W = 100$ MHz).

single channel (see Fig. 1-a). It is effective under small BS/UE density where SIR is low, yielding FR_b 's smaller interferer density normalized by BS density λ_i^*/λ_b . Note also that non-smooth FR_b and FR_u curves in Figs. 5 and 6 are because M_b and M_u are integers as elaborated in Remark 3.

VII. CONCLUSION

In this paper we derive closed-form ubiquitous rate, and investigate two frequency reuse schemes FR_b and FR_u so that they can ubiquitously achieve the UR2C's target 50 Mbps data rate with 99% SIR reliability. Both of their optimal designs provide higher ubiquitous rates compared to the baseline without frequency reuse. This result is different from traditional network design guidelines that prefer not to use frequency reuse for only maximizing data rate without guaranteeing reliability. To enable UR2C, it would also be interesting to revisit other reliability achieving schemes such as double associations for attaining diversity gain [11].

APPENDIX

Proof of Lemma 3: Let $f(x) = {}_2F_1(1, -\frac{2}{\alpha}; 1 - \frac{2}{\alpha}; -x)^{-1}$. By the Gauss-hypergeometric function definition,

$$f(x) = \left[\sum_{n=0}^{\infty} \frac{(1)_n \left(-\frac{2}{\alpha}\right)_n (-x)^n}{\left(1 - \frac{2}{\alpha}\right)_n n!} \right]^{-1} = 1 - \frac{2x}{\alpha - 2} + O(x^2) \quad (19)$$

The last step follows from Taylor's expansion for $x \rightarrow 0$. This indicates $\lim_{x \rightarrow 0} f'(x) = -2/(\alpha - 2)$.

Consider $g(x) := (1+x)^{-\frac{2}{\alpha-2}}$, having the same slope as $f'(x)$ as $x \rightarrow 0$. To verify $g(x) \leq f(x)$, we consider the first and second derivatives of $f(x)$ and $g(x)$ for $x > 0$ as follows:

$$f'(x) = -\frac{2[f(x) - (1+x)^{-1}f(x)^2]}{\alpha x}; \quad (20)$$

$$f''(x) = \frac{2(2+\alpha) + (1+x)^{-2}[8 - 2(\alpha+6+6x+2\alpha x)f(x)]}{(\alpha x)^2 f(x)^2}; \quad (21)$$

$$g'(x) = -\frac{2(1+x)^{-\left(1+\frac{\alpha}{\alpha-2}\right)}}{\alpha-2}; \quad g''(x) = \frac{2\alpha(1+x)^{-2\left(1+\frac{\alpha}{\alpha-2}\right)}}{(\alpha-2)^2}. \quad (22)$$

Firstly, $f'(x), g'(x) < 0$, $f''(x) > 0$, and $g''(x) \geq 0$ for all $x > 0$ where the equality holds when $x \rightarrow \infty$ and/or $\alpha \rightarrow \infty$. Secondly, $\lim_{x \rightarrow 0} f'(x)/g'(x) = 1$ and $\lim_{x \rightarrow \infty} f'(x)/g'(x) \leq 1$ where the equality holds when $\alpha \rightarrow \infty$. Lastly, $f(0)/g(0) = 1$ and $\lim_{x \rightarrow \infty} f(x)/g(x) = 1$ due to their original coverage probability definitions. As x increases, these conclude that $f(x)$ and $g(x)$ are monotonically decreasing, starting identically from unity while the decreasing slope of $g(x)$ is steeper than that of $f(x)$ due to $f'(x)/g'(x) \leq 1$ for all $x > 0$. This concludes the proof of $f(x) \geq g(x)$ for all x . ■

Proof of Proposition 2: Let a_i denote $p_c(\lambda_b)/M_b$, $p_c(\lambda/M_u)$, and $p_c(\lambda)$ respectively for FR_b , FR_u and the baseline. By applying Proposition 1, the reliability constraint equation $\mathcal{P}_t(M_i) = \eta$ is rephrased with respect to t as $t = a_i^{-\frac{\alpha}{2}} [\eta^{-\left(\frac{\alpha}{2}-1\right)} - 1] = a_i^{-\frac{\alpha}{2}} [1 - (1-\eta)]^{-\left(\frac{\alpha}{2}-1\right)} - 1$ (23)

In (23), applying Taylor expansion for $\eta \approx 1$ makes $[1 - (1-\eta)]^{-\left(\frac{\alpha}{2}-1\right)}$ become $1 + c_\eta$. Applying this with Table II and a typical UE's reliability η to (2) provides the desired result. ■

Proof of Proposition 3: According to Karush-Kuhn-Tucker (KKT) first and second order conditions, the local maximum of $\mathcal{R}_\eta(M_b)$ in (13) is the global maximum. Likewise, the local maximum of $\mathcal{R}_\eta(M_u)$ in (14) becomes its global maximum. Therefore, M_b and M_u can maximize $\mathcal{R}_\eta(M_b)$ and $\mathcal{R}_\eta(M_u)$ when respectively satisfying the first order conditions $d\mathcal{R}_\eta(M_b)/dM_b = 0$ and $d\mathcal{R}_\eta(M_u)/dM_u = 0$. Now that M_b and M_u are integers no smaller than 1, the values minimizing the LHS of the first order conditions provide the optimal numbers of channels, finalizing the proof. ■

REFERENCES

- [1] N. Alliance, "Recommendations for NGMN KPIs and Requirements for 5G," Jun. 2016.
- [2] Qualcomm, "5G Vision Presentation," Feb. 2016.
- [3] P. Popovski, "Ultra-Reliable Communication in 5G Wireless Systems," in *Proc. 1st Int. Conf. on 5G for Ubiquitous Connectivity (5GU)*, Levi, Finland, Nov. 2014.
- [4] J. Park, S.-L. Kim, and J. Zander, "Tractable Resource Management with Uplink Decoupled Millimeter-Wave Overlay in Ultra-Dense Cellular Networks," *IEEE Trans. Wireless Commun.*, vol. 15, pp. 4362–4379, Jun. 2016.
- [5] J. G. Andrews, F. Baccelli, and R. K. Ganti, "A Tractable Approach to Coverage and Rate in Cellular Networks," *IEEE Trans. Commun.*, vol. 59, pp. 3122–3134, Nov. 2011.
- [6] X. Zhang and M. Haenggi, "A Stochastic Geometry Analysis of Inter-Cell Interference Coordination and Intra-Cell Diversity," *IEEE Trans. Wireless Commun.*, vol. 13, pp. 6655–6669, Dec. 2014.
- [7] M. Haenggi, *Stochastic Geometry for Wireless Networks*. Cambridge Univ. Press, 2013.
- [8] S. M. Yu and S.-L. Kim, "Downlink Capacity and Base Station Density in Cellular Networks," *Proc. IEEE WiOpt Wksp. on Spatial Stochastic Models for Wireless Networks (SpaSWiN)*, May 2013.
- [9] D. Stoyan, K. W. S., and J. Mecke, *Stochastic Geometry and its Applications*. Wiley, 2nd ed., 1995.
- [10] G. E. Andrews, R. Askey, and R. Roy, *Special Functions*. Cambridge Univ. Press, 1999.
- [11] D. M. Kim and P. Popovski, "Reliable Uplink Communication through Double Association in Wireless Heterogeneous Networks," *IEEE Wireless Commun. Lett.*, vol. 5, pp. 312–315, Jun. 2016.